Oxford University
Atmospheric, Oceanic and Planetary Physics Department

MODELLING THE VERTICAL DISTRIBUTION OF SULFUR DIOXIDE IN VOLCANIC PLUMES USING IASI MEASUREMENTS

Isabelle Wright
August 2023

Supervisor: Anu Dudhia

Abstract

Within this project, IASI measurements have been used to model the vertical distribution of sulfur dioxide in volcanic plumes. The original retrieval models the SO_2 spread throughout the atmosphere taking information from the a-priori estimates and covariance matrix used. By making edits to the correlation length within the covariance matrix, the variance of the a-priori estimate and which profiles are being retrieved, the model was improved to recognise the SO_2 as a layer. The improved retrieval was then compared to an alternative retrieval method, which had been previously developed. Some variations between the two were identified, however there were some clear trends between the two retrievals.

1 Introduction

Sulfur dioxide (SO_2) is an important gas within our atmosphere due to its effects in both the troposphere and stratosphere. In the troposphere, it can cause acidification of rainfall, modification of cloud formation and impacts air quality and vegetation. In the stratosphere, the SO_2 oxidises, forming H_2SO_4 aerosol, affecting the climate for several years. Atmospheric SO_2 also impacts air safety due to the sulfidation of the nickel alloys within aircraft engines, corroding them. Volcanic eruptions are a significant source of atmospheric SO_2, contributing to about one-third of the tropospheric sulfur burden. The effects from the SO_2 emitted depend not only on the concentration in the atmosphere, but also the altitude. (Carboni, 2016)

Volcanic SO_2 emissions have been widely studied using ground based UV instruments. However, ground based techniques are not widely available at remote regions. Where they are available, the measurements are limited to daytime monitoring, and they are not effective when tracking plumes over large geographic areas. Satellite monitoring offers a cost effective technique which solves some of the limitations associated with ground-based monitoring. The advances within this technology over the past few decades allow volcanic activity to be monitored from space, including the detection and retrieval of SO_2. (Taylor, 2018)

Within this project, satellite measurements from IASI were used to model the vertical distribution of SO_2 within volcanic plumes. The retrieval was edited to encourage it to recognise the SO_2 as a layer within the plume, rather than assuming the SO_2 is spread throughout the atmosphere.

2 Method

2.1 IASI Data

The Infrared Atmospheric Sounding Interferometer (IASI) is onboard the MetOp A, B and C satellites, launched in 2006, 2012 and 2018 respectively. IASI is an advanced Fourier transform spectrometer coupled with an infrared imager, which measures across the spectral range 645 to 2760 cm^{-1} with a spectral resolution of 0.5 cm^{-1}. Each scan provides a swath width of 2200 km, composed of circular fields-of-view with radius 12km. The satellites follow the same orbit, with 50 minutes between the two, meaning they have near-global coverage every 12 hours. Given the spectral range and resolution, along with the geographical coverage, IASI is well suited for monitoring atmospheric composition. (Walker, 2011)

IASI can measure volcanic SO_2 in three spectral regions; $\upsilon_1 + \upsilon_3$ is located at 4.0μm, υ_3 is located at 7.3μm, and υ_1 is located at 8.7μm. The $\upsilon_1 + \upsilon_3$ band is weak and only used when large amounts of SO_2 saturates the other absorption bands. The υ_3 band is the strongest of the three, but is collocated with a strong water absorption band, consequently reducing its sensitivity to SO_2 emission from the surface and lower atmospheric levels. The υ_1 band is a region of relatively high transmittance, containing information on the SO2 amount for lower tropospheric

plumes. However, this band does not contain significant spectral information on the plume altitude. (Carboni, 2012).

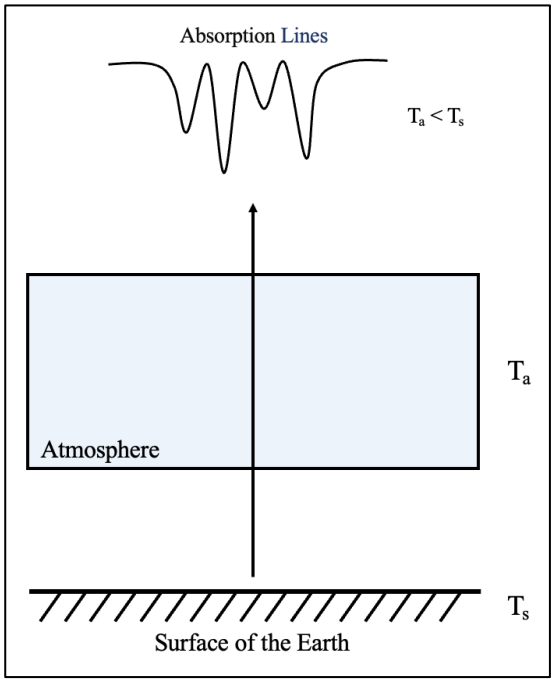

Figure 1 *A diagram illustrating the process leading to the brightness temperature spectrum. T_s is the temperature of the surface, T_a is the temperature of the atmosphere.*

Figure 1 shows a simplified diagram illustrating the process leading to the brightness temperature spectrum. The satellite makes the measurements, and if the temperature of the atmosphere, T_a, is lower than the temperature of the surface of the Earth, T_s, the brightness temperature spectrum will show absorption lines. Similarly, if the T_a is lower than T_s, the spectrum will have transmittance lines.

Figure 2 shows the brightness temperature spectrum for the main atmospheric components. Within this spectrum, only major contributors are visible due to their high absorption. In figure 3, the smaller contributors are replotted, where SO_2 is visible. The 2 bands used for this retrieval were the υ_1 and υ_3 absorption bands. These are both visible in figure 3 in the wavenumber ranges 1130 – 1200 cm^{-1} and 1340 – 1380 cm^{-1}. Within figure 2, it is clear that there is a strong water absorption band where the υ_3 absorption band is, and there is a region of relatively high transmittance for the SO_2 around the υ_1 absorption band.

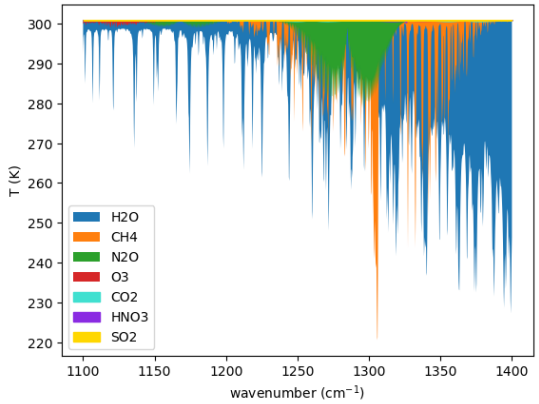

Figure 2 *The brightness temperature plotted against wavenumber for the main components of the atmosphere.*

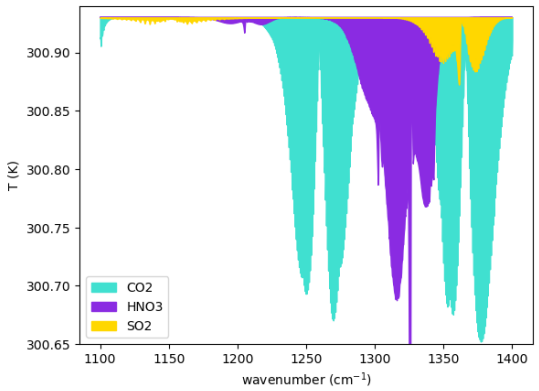

Figure 3 *The brightness temperature plotted against wavenumber for the 3 smaller contributors within the atmosphere.*

2.2 Iterative Optimal Estimation Retrieval

An iterative optimal estimation retrieval was used. This retrieval makes use of both

the υ_1 and υ_3 absorption bands to retrieve the SO_2 amounts and pressure. The scheme iteratively fits the forward model with the measurements, using the error covariance matrix in order to seek a minimum cost function.

Covariance is the idea that two uncertainties are related and can affect one another. The optimal estimation form, where we wish to include a-priori information to constrain the fit, is

$$\chi^2 = \left(\mathbf{K^T S_y^{-1} K} + \mathbf{S_a^{-1}}\right)^{-1}(\mathbf{K^T S_y^{-1} y} + \mathbf{S_a^{-1} x_a})$$

$\boldsymbol{x_a}$ are the a-priori values, $\boldsymbol{S_a}$ is the a-priori covariance matrix, $\boldsymbol{K}$ is the Jacobian matrix, $\boldsymbol{S_y}$ is the error covariance matrix, and $\boldsymbol{y}$ is a vector representing the measured values (Rogers, 2000).

The purpose of the a-priori is to ensure the matrix inversion is possible, even when the measurements have little or no unique sensitivity to the retrieved parameters. If the measurement knowledge was reliable and the a-priori estimate was poor, then the equation would reduce to the least squares solution for the fit. However, if there is a lot of noise, giving large values in the elements of the error covariance matrix, $\boldsymbol{S_y}$, the least squares fitting equation without the presence of the a-priori will almost certainly fail due to the degeneracy. The inclusion of the a-priori covariance matrix, $\boldsymbol{S_a}$, allows the matrix to be inverted, improving the stability.

To simplify the model, assume that a 2-level profile is being retrieved, meaning a 2x2 a-priori covariance matrix is being used. The diagonal elements are the variances of the a-priori estimate. If the a-priori profile had 100% uncertainty and no correlation between the values, the value at one level tells you nothing about the value at an adjacent level, giving the least informative version. If the off-diagonal elements of the 2x2 matrix are positive, if the a-priori is high at one level, it is likely to be high at another level. Similarly, if the off diagonal elements are negative, if the a-priori is high at one level, it is likely to be low at another level. Within this project, these correlations represent departures of the actual SO_2 profile from the low background state, so are always positive and decay away from the diagonal of S_a with a lengths scale representing the half- width of the plume. Reducing the diagonal elements and/or adding corelation to the off-diagonal elements both act to add to the information supplied from the a-priori compared to that from the measurements.

3 Results

3.1 The 2018 Eruption of Sierra Negra

The case study selected to test the retrieval was the 2018 eruption of Sierra Negra, on Isla Isabela, within the Galápagos Islands. Sierra Negra has experienced at least 7 eruptions since 1911, with an eruption occurring approximately every 15 years. The 2018 eruption occurred on 26 June and lasted 58 days, covering a 30.6 km^2 area in fresh lava. (Gregg, 2022). The IASI data used was a single orbit from 27 June, capturing the beginning of the eruption.

3.2 Recognising the SO_2 as a Layer

Figure 4 shows the Baseline which any edits to the retrieval are compared to. In the absence of reliable information on the actual distribution of SO_2, an ad hoc assumption was made that if a feature could be reliably reproduced with the retrieval run at different vertical spacings, it was more likely to represent the 'real' atmospheric distribution of SO_2.

As seen in figure 4, the SO_2 is vertically spread throughout the atmosphere, with no clear layer indicating the height of the plume. This is a result of the retrieval becoming too reliant on the a-priori estimate. The a-priori is based on the equilibrium atmospheric levels, assuming that the SO_2 is spread evenly throughout the atmosphere. In order to encourage the retrieval to recognise the SO_2 as a layer, it has to become less reliant on the a-priori estimate, without becoming too unstable.

In order to improve the Baseline, a range of improvements were made. Within the Baseline, the temperature and water vapour profiles are fixed from the climatological values. To improve this, Eumetsat retrieved profiles, which are likely to be more representative of the true conditions, were used. Temperature and water vapour profiles were added to the list of profiles being retrieved to further refine them. To improve the temperature profile, the CO_2 band, at 680 – 690 cm^{-1} wavenumbers, was included. The correlation length was changed to 2km for the SO_2 retrieval, meaning more information was supplied by the measurements, as opposed to the a-priori. The correlation length was decreased further, however this caused significant variations between the different vertical spacings, suggesting the retrieval did not have enough information from the a-priori estimate, making it unstable. In order to counteract this, the percentage uncertainty was decreased in an attempt to increase the information taken from the a-priori. However, this did not improve the retrieval enough, making it safe to assume the previous edits gave the optimum retrieval.

The improved retrieval can be seen in figure 5. In order to compare with the baseline, the same 4 pixels were plotted for the same 3 vertical spacings. In figure 5, it is clear that the model has improved, and the retrieval is now recognising the SO_2 as a distinct layer. It is no longer spread throughout the atmosphere and is now only present in a clear altitude.

In the improved retrieval, in figure 5, there is still some variation between the different vertical spacings. This is most likely because the retrieval relies on the a priori more if there are a greater number of points to retrieve. Given the different number of points needed for the different spacings, there will be some variation. However, when comparing to the baseline, it is reasonable to say that the different vertical spacings now agree.

3.3 Mapping the plume

Maps of the retrieved heights and column amounts can be seen in figure 6 and figure 9 respectively. It was assumed that any pixels with column amounts below 0.002 ppmv are due to background SO_2 and are

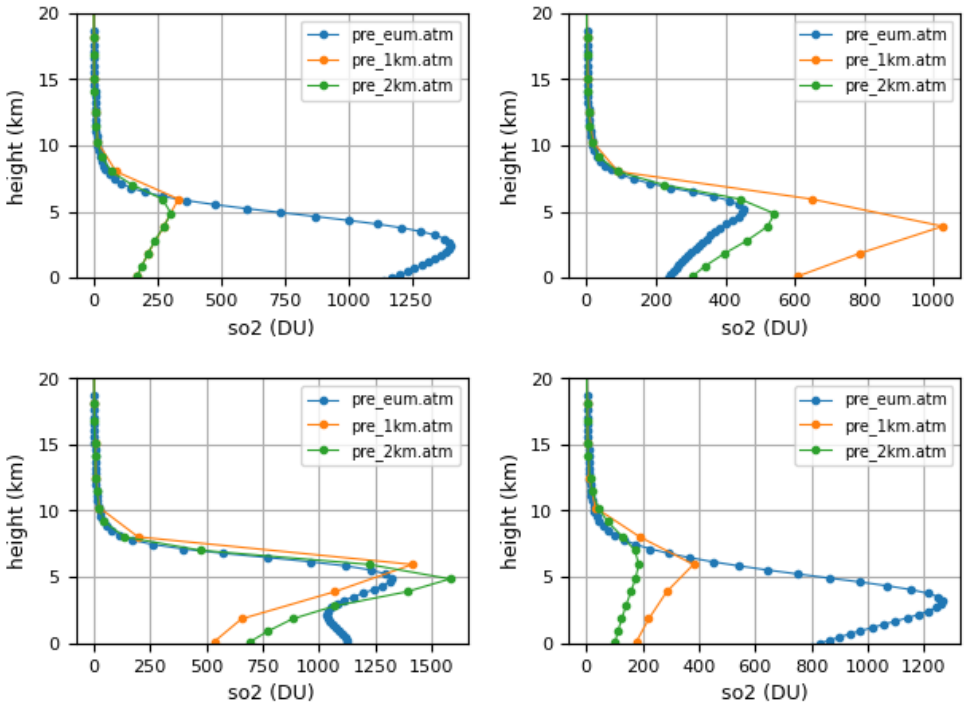

Figure 4 *4 pixels were identified within the plume to act as a Baseline to compare any further changes to the retrieval with. For the Baseline, the surface temperature, SO_2 and H_2O profiles were retrieved. The regions between 1130 – 1200 cm^{-1} and 1340 – 1380 cm^{-1} were used, which contained the ν_1 and ν_3 bands. The Baseline covariance matrix settings had a percentage standard deviation of 100% with a correlation length of 50km.*

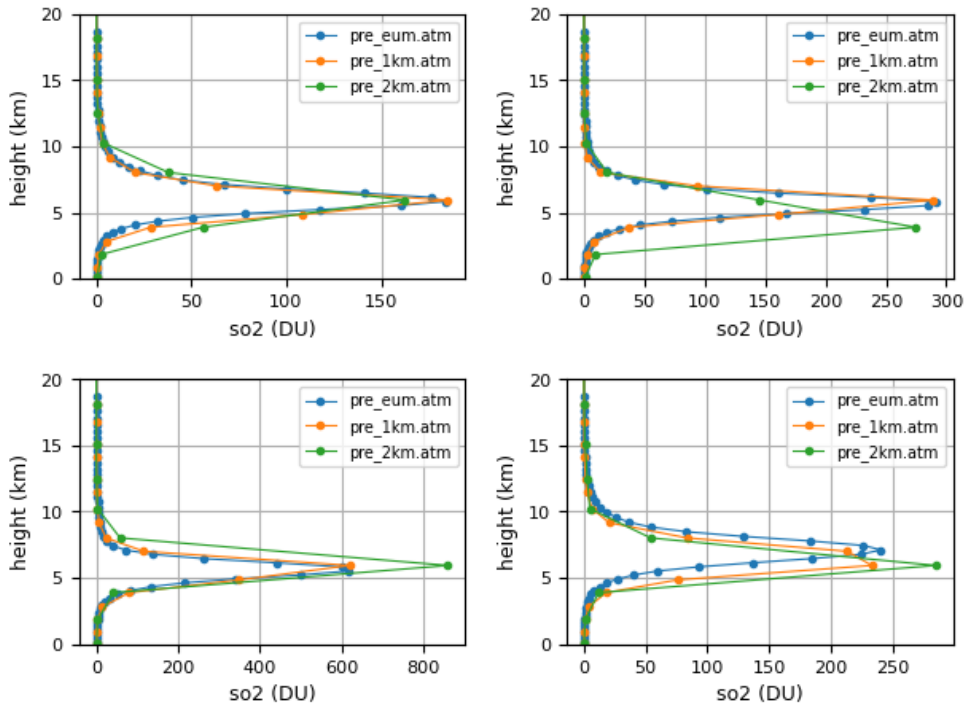

Figure 5 *The same 4 pixels as used in the Baseline were plotted using the improved retrieval.*

not within the plume. Hence, any pixels with low SO_2 column amounts were removed.

Figure 6 shows a map of the retrieved heights for each pixel. By plotting the plume heights on a map, it can be used to ensure the retrieval works consistently across all the pixels. This can be seen in the smooth change in heights across the plume. The further away from the volcano, the higher the plume becomes. There is also an area around at 94.6°W 2.8°S where the plume has much smaller heights than the rest.

Figure 7 shows the map of the retrieved heights for the Iterative retrieval, developed by Isabelle Taylor. For the comparison, the retrieval used within this project will be referred to as the Morse retrieval, and the alternative retrieval, developed by Isabelle Taylor, will be referred to as the Iterative retrieval. When comparing the 2 plots, the Iterative retrieval has much smaller heights than figure 6. In addition to this, the lower heights present in figure 6, around 94.6°W 2.8°S, are not present in figure 7. The Iterative retrieval relies more heavily on the a-priori estimate, whilst the retrieval which is used within this project relies more on the measurements. This could have led to the more uniform and lower heights seen in figure 7.

Looking more closely at the comparison between the 2 retrieval methods, figure 8 shows the 2 height profiles plotted against each other. There is a linear relationship between the 2 retrievals, however there is also a spread around this correlation. The

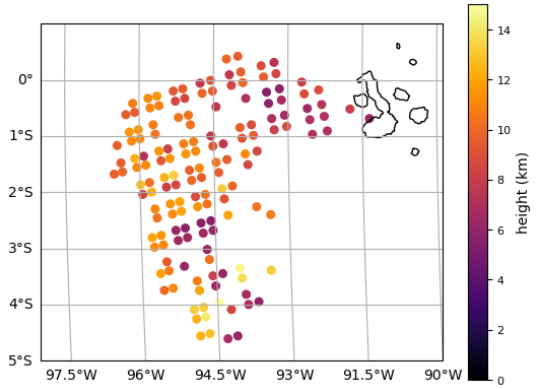

Figure 6 *A colour map illustrating the height in km of each pixel on a longitude vs latitude plot. This was the height profiles obtained for the retrieval developed in this project, known as the Morse retrieval.*

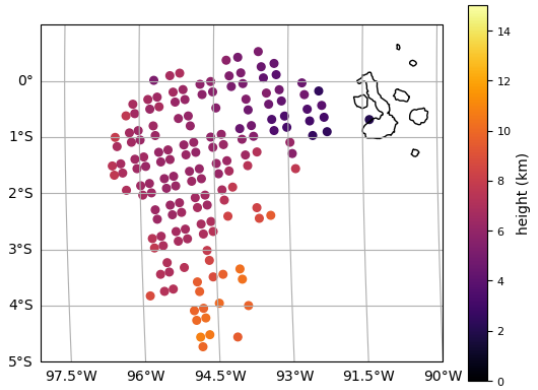

Figure 7 *A colour map illustrating the height in km of each pixel on a longitude vs latitude plot. This was the height profiles obtained for the alternative retrieval used to compare with this project, known as the Iterative retrieval.*

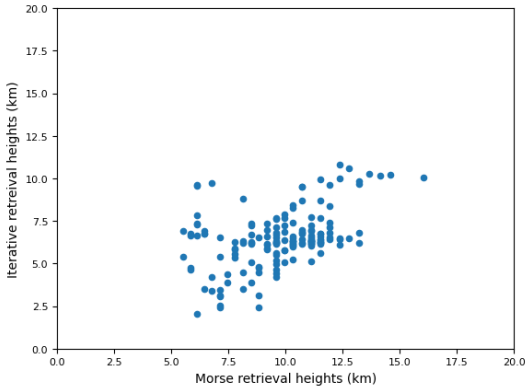

Figure 8 *The height profiles for the morse retrieval and the iterative retrieval plotted against each other.*

Morse retrieval has larger values in comparison to the Iterative retrieval, at around 4-5km larger. The height profiles for the Iterative retrieval tend towards values in a range 5-7 km, which is is clear where the values are focussed around a horizontal line through 6km. This has happened because the Iterative retrieval is more reliant on the a-priori estimate, making the height profile much closer to this estimate, around 5-7 km, rather than the measurements.

The Morse retrieval, in figure 6, contains heights at a much lower value than expected, around 94.6°W 2.8°S, which is not seen in the Iterative retrieval, in figure 7. This is also seen in figure 8 where there are some outliers which do not match the overall trend in values.

Figures 9 and 10 show maps of the SO_2 column amount profiles for the 2 different retrievals. The Morse retrieval has no clear trend in the data, whilst the Iterative retrieval has higher SO_2 column amounts closer to the island, which decrease as the plume moves away from the volcano. The Morse retrieval is also missing the distinct feature of the high SO_2 closest to the volcano as seen in the Iterative retrieval. Both have another area of high SO_2 later in the plume around 94.6°W 2.8°S, which agree with the location of the lower heights given by the Morse retrieval.

Figure 11 shows the comparison between the 2 retrieval methods by plotting them against each other. There are 3 different linear relationships between the two profiles. In addition to this, the column amounts for the Iterative retrieval

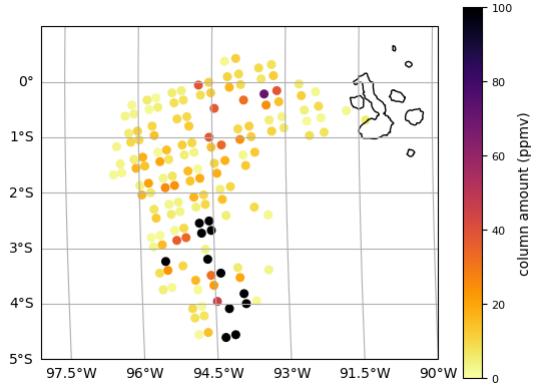

Figure 9 *A colour map illustrating the SO_2 column amounts in DU of each pixel on a longitude vs latitude plot. This was the SO_2 profiles obtained for the retrieval developed in this project, known as the Morse retrieval.*

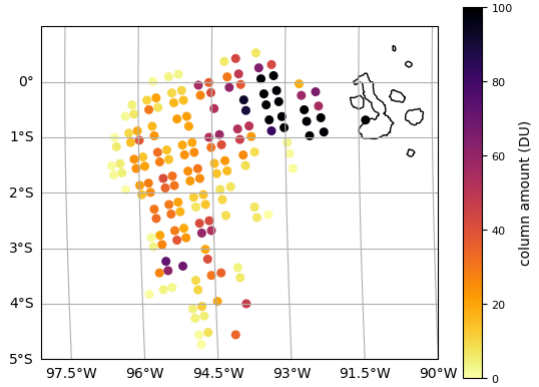

Figure 10 *A colour map illustrating the SO_2 column amounts in DU of each pixel on a longitude vs latitude plot. This was the SO_2 profiles obtained for the alternative retrieval used to compare with this project, known as the Iterative retrieval.*

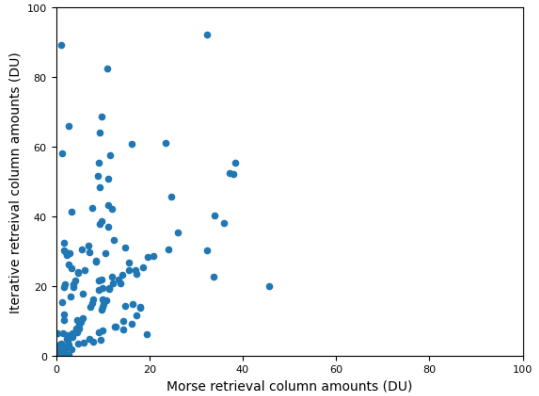

Figure 11 *The SO_2 column amount profiles for the morse retrieval and the iterative retrieval plotted against each other.*

range from 0 to 100 DU, whereas the Morse retrieval ranges from 0 to 50 DU. There are some higher amounts as seen in figure 9, however in figure 11, the x-axis is limited to 100 as these values around 4.6°W 2.8°S are much larger and would make any trends in the data difficult to identify. These anomalies could be due to the retrieval starting to become unstable as it is becoming less reliant on the a-priori. These higher SO_2 column amounts are in a similar location to the lower heights, suggesting there could be a correlation here.

Further research would be required to determine which retrieval method would be more reliable. Although the Morse retrieval relies more on the measurements as opposed to the a-priori estimate, this makes the retrieval more unstable, which could lead to inaccurate results.

4 Conclusion

The Baseline retrieval was improved by adding temperature and water vapour profile retrievals, including the Eumetsat retrieved profiles and by changing the corelation length of the covariance matrix to 2km. The improved retrieval shows a distinct layer, where all three vertical spacings agree with each other. By decreasing the correlation length any further, the three vertical spacings no longer agreed, suggesting the retrieval becomes unstable at any smaller correlation lengths than 2 km. Changing the percentage variance made no significant improvements to the retrieval.

When both the height and SO_2 column amounts are plotted, a distinct plume is seen. There are correlations between the Morse retrieval and alternative Iterative retrieval, however some variations between the two have been identified. There was an area of lower heights that was only seen on the Morse retrieval around 4.6°W 2.8°S. At this same location on both retrievals there was an area of high SO_2 column amounts. Further research would be needed to be completed to determine whether this is meant to be present and therefore which retrieval is more accurate.

5 References

E. Carboni R. Grainger, J. Walker, A. Dudhia, R. Siddans A new scheme for sulfur dioxide retrieval from IASI measurments: application to the Eyjafjallajokull eruption of April and May 2010 [Journal] // Atmospheric Chemistry and Physics. - 2012. - pp. 11417-11434.

E. Carboni R. Grainger, J. Walker, A. Dudhia, R. Siddans A new scheme for sulfur dixide retreival for IASI measurements: application to the Eyjafjallajokull erruption of April and May 2010 [Journal]. - 2012.

Elisa Carboni Roy G. Granger, Tamsin A. Mather, David M. Pyle, Gareth E. Thomas, Richard Siddans, Andrew J. A. Smith, Anu Dudhia, Mariliza E. Koukouli, Dimitrios Balis The vertical disstribution of volcanic SO2 plumes measured by IASI [Journal]. - 2016.

Elisa Carboni Roy G. Granger, Tamsin A. Mather, David M. Pyle, Gareth E. Thomas, Richard Siddans, Andrew J. A. Smith, Anu Dudhia, Mariliza E. Koukouli, Dimitrios Balis The vertical distribution of volcanic SO2 plumes measured by IASI [Journal] // Atmospheric Chemistry and Physics. - 2016. - pp. 4343-4367.

Isabelle A. Taylor James Preston, ELisa Carboni, Tamsin A. Mather, Roy G. Granger, Nicolas Theys, SIlvana Hidalgo, Brendan McCormick KIlbride Exploring the Uitility of IASI for monitoring Volcanic SO2 Emissions [Journal]. - 2018.

Isabelle A. Taylor James Preston, ELisa Carboni, Tamsin A. Mather, Roy G. Granger, Nicolas Theys, SIlvana Hidalgo, Brendan McCormick KIlbride Exploring the Utility of IASI for monitoring Volcanic SO2 Emissions [Journal] // Journal of Geophysical Research: Atmospheres. - 2018. - pp. 5588-5606.

J.C. Walker A. Dudhia, E. Carboni An effective method for the detection of trace species demonstated using the MetOP Infrared Atmospheric Sounding Inferometer [Journal]. - 2011.

J.C. Walker A. Dudhia, E. Carboni An effective method for the detection of trace species demonstrated using the MetOp Infrared Atmospheric Sounding Interferometer [Journal] // Atmospheric Measurement Techniques. - 2011. - pp. 1567-1580.

Patricia M. Gregg Yan Zhan, Falk Amelung, Dennis Geist, Patricia Mothes, Seid Koric, Zhang Yunjun Forecasting mechanical failure and teh 26 June 2018 eruption of Sierra Negra Volcano, Galapagos, Ecuador [Journal]. - [s.l.] : Science Advances, 2022. - 22 : Vol. 8.

Rogers Clive D. Inverse Methods for Atomspheric Sounding Theory and Practice [Book]. - [s.l.] : World Scientific Publishing co. , 2000. - Vol. Vol. 2.